

## Optical gain and stimulated emission in silicon nanocrystals

L. Dal Negro<sup>a</sup>, M. Cazzanelli<sup>a</sup>, Z. Gaburro<sup>a</sup>, P. Bettotti<sup>a</sup>, L. Pavesi<sup>a</sup>

D. Pacifici<sup>b</sup>, G. Franzò<sup>b</sup>, F. Priolo<sup>b</sup> and F. Iacona<sup>c</sup>

<sup>a</sup> INFN-Dipartimento di Fisica, via Sommarie 14, Università di Trento, I-38050 Povo (Trento), Italy

<sup>b</sup> INFN-Dipartimento di Fisica, Università di Catania, I-95129 Catania

<sup>c</sup> CNR-IMM, Sezione di Catania, I-95121 Catania, Italy

### ABSTRACT

Time-resolved luminescence measurements on silicon nanocrystal waveguides have revealed a fast recombination dynamics, related to population inversion which leads to net optical gain. The waveguide samples were obtained by thermal annealing of plasma enhanced chemical vapour deposited thin layers of silicon rich oxide. Variable stripe length measurements performed on the fast emission signal have shown an exponential growth of the amplified spontaneous emission, with net gain values of about  $10 \text{ cm}^{-1}$ . Both the fast component intensity and its temporal width revealed threshold behaviour as a function of the incident pump intensity. A modelling of the decay dynamics is suggested within an effective four level rate equation treatment including the delicate interplay among stimulated emission and Auger recombinations.

### INTRODUCTION

One goal for silicon microphotronics consists in the demonstration of a laser device based on silicon [1,2]. Following the initial observations of optical gain in highly packed silicon nanocrystals (Si-nc) prepared by ion-implantation [3], other works have recently demonstrated the possibility of stimulated emission in Si-nc [4-6]. Nanosecond gain dynamics [4] and evidences for speckle patterns [5] in the spatially coherent emission have been recently reported.

As in other quantum dot based systems [7,8], a severe competition with efficient non-radiative processes, mainly Auger type, is present in Si-nc, which causes very fast dynamics in the optical gain. Although a clear understanding of the microscopic gain mechanism is still under debate, it has been realised that interface radiative states associated with oxygen atoms can play a crucial role in determining the emission properties of the Si-nc systems [9,10]. Here we report on light amplification dynamic studies in Si-nc and we propose a simple phenomenological model to explain our experimental results.

### TIME RESOLVED VARIABLE STRIPE LENGTH RESULTS

We studied Si-nc samples produced by high temperature annealing of substoichiometric silicon oxide ( $\text{SiO}_x$ ) thin films grown by plasma enhanced chemical vapour deposition (PE-CVD) on a quartz substrate. The structural and luminescence properties of these systems have been fully discussed elsewhere [11]. Here we focus on a representative sample produced with a total Si content of 42 at.% and with an annealing temperature of  $1250 \text{ }^\circ\text{C}$  for one hour which yields closely packed Si-nc with a mean diameter of 1.7 nm. The Si-nc rich layer (250 nm thick) was embedded between two 100 nm thick  $\text{SiO}_2$  layers to form an optical waveguide. Considering the

measured refractive index of 1.82, the optical confinement factor of the waveguide was estimated to be 74 %. To investigate the stimulated emission dynamics, time-resolved experiments were performed in the one dimensional amplifier configuration (pumping through the surface and collection of the guided light from one edge of the sample). This approach, also called variable stripe length (VSL) method [12], allows to measure the stimulated emission build-up time as the signal photons propagate along the amplification axis (amplified spontaneous emission, ASE). Although simple in principle, VSL techniques applied to Si-nc can present some experimental difficulties which have been fully characterised elsewhere [13,14]. High fluence ( $J_p$ ) short optical pulses (6 ns, 10 Hz, 355 nm) produced by the third harmonic of a Nd-YAG pulsed laser were used to excite the samples. Care has been used to keep the fluence lower than the sample damage threshold. A single grating spectrometer and a visible streak camera have been used to detect the time resolved signal. When the VSL configuration was used, edge emission was collected by a 20X optical microscope objective with a numerical aperture of 0.3 larger than the output numerical aperture of the waveguide sample. This allows constant collection efficiency over the whole pumping length.

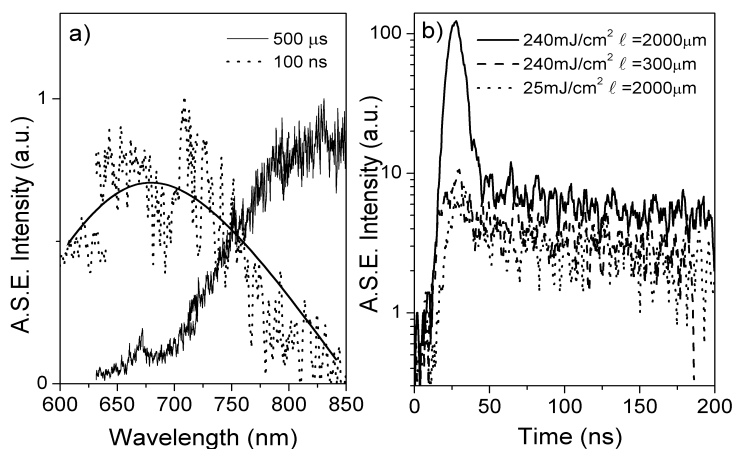


Figure 1. (a) Time resolved amplified spontaneous emission (A.S.E.) spectra integrated over 100 ns (dashed line) or 500  $\mu$ s (full line). A pumping length  $\ell=2$ mm, fluence of 240 mJ/cm<sup>2</sup>, laser wavelength 355 nm were used. (b) Pumping length  $\ell$  and pumping fluence dependence of A.S.E. time decay.

Figure 1a shows the time resolved ASE spectra at two observation time scales. For long integration times of 500  $\mu$ s the usual broad emission lineshape centred at 900 nm is measured. This emission has similar spectral feature as the usual luminescence from Si-nc [11]. On the contrary, when the first 30 ns are considered, a fast recombination component appears in the decay dynamics (Fig. 1b) and the spectral shape of the ASE signal is blue shifted at 700 nm. The fast component disappears when either the excitation length  $\ell$  is decreased at a fixed  $J_p$  or when  $J_p$  is decreased for a fixed  $\ell$  (Fig. 1b). In addition the peak intensity of the fast component shows a super linear increase vs  $\ell$  for high  $J_p$  which can be fitted with the usual one-dimensional amplifier equation [15] yielding a net optical gain of  $12 \pm 3$  cm<sup>-1</sup> at 760nm (Fig. 2a). Modal gain values ranging between 8 cm<sup>-1</sup> and 20 cm<sup>-1</sup> are measured depending on the detection wavelength. When the same fit is performed on the slow component, optical losses of about 20-30 cm<sup>-1</sup> can be extracted. In addition, the fast component peak intensity shows a threshold behaviour vs  $J_p$  (Fig. 2b): at low  $J_p$  the emission is sublinear to a power 0.5 in a double logarithmic scale suggesting a

strong Auger limited regime [16], while for higher  $J_p$  population inversion is achieved and a superlinear increase to a power  $\approx 3$  is measured, suggesting the onset of the stimulated regime. Moreover, the full width at half maximum FWHM of the fast component signal decreases significantly when the stimulated regime is entered (Fig. 2b).

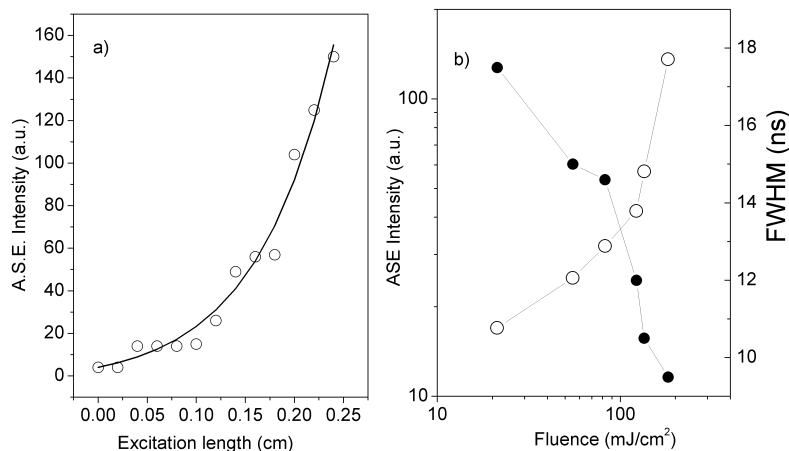


Figure 2. (a) Amplified spontaneous emission (ASE) peak intensity (circles) versus the excitation length for a wavelength of 760nm and pump fluence of 200mJ/cm<sup>2</sup>. The full line is a fit of the data with the one-dimensional amplifier model which yields a net modal gain values of  $12 \pm 3 \text{ cm}^{-1}$ . (b) ASE peak intensity and full width half maximum (FWHM) of the fast component versus the pumping fluence. The pumping length is fixed at  $\ell = 2\text{mm}$ .

Fast component in the luminescence decay of heavily photo excited porous silicon has been attributed to Auger recombinations [16,17]. Auger recombinations can explain the appearance of a fast non radiative recombination at high pumping rates, but not the superlinear increase of the VSL signal as a function of  $\ell$  and as a function of  $J_p$ , nor the significant shortening of the emission temporal profile when stimulated emission sets in.

## RATE EQUATION MODELING

These experimental data (Fig. 1 and 2) supports a phenomenological model based on a four level system where a strong competition between fast Auger processes and stimulated emission is considered. The following set of rate equations describes the model:

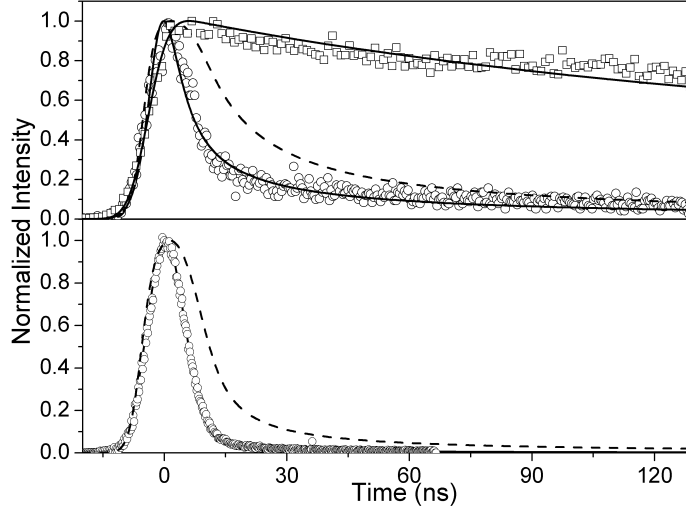


Figure 3. (Top) Time decay of the photoluminescence signal measured at 0.4 mJ/cm<sup>2</sup> (open squares) and at 1 mJ/cm<sup>2</sup> (open circles). Pumping wavelength was 430 nm. The solid lines are the simulations of the emitted photon obtained by solving the set of rate equations with the following parameters:  $C_A=50 \times 10^{11}$  cm<sup>3</sup>s<sup>-1</sup> (yielding an Auger lifetime of 6 ns at the peak fluence),  $\phi_p=3 \times 10^{20}$  photons s<sup>-1</sup>cm<sup>-2</sup> and  $\phi_p=3 \times 10^{23}$  photons s<sup>-1</sup>cm<sup>-2</sup>,  $\sigma_p=10^{-15}$  cm<sup>2</sup>,  $\sigma=10^{-17}$  cm<sup>2</sup>,  $N=6 \times 10^{17}$  cm<sup>-3</sup>,  $\beta=4.5 \times 10^{-4}$ ,  $\alpha=3$  cm<sup>-1</sup>,  $1/\tau=10^6$  s<sup>-1</sup>,  $\Gamma_{43}=\Gamma_{21}=10^{15}$  s<sup>-1</sup>,  $1/\tau_R=10^3$  s<sup>-1</sup> and  $d=10^{-4}$  cm. The dashed line is the simulation when the stimulated emission is neglected while  $C_A=30 \times 10^{11}$  cm<sup>3</sup>s<sup>-1</sup> to have an Auger lifetime of 6.46 ns at peak fluence as in the other simulation. (bottom) Luminescence decay (open circles) at a pumping fluence of 15 mJ/cm<sup>2</sup>. The lines are simulations with (full line) or without (dashed line) positive optical gain with the same parameters as in the top panel except for  $\phi_p=3 \times 10^{24}$  photons s<sup>-1</sup>cm<sup>-2</sup> and  $C_A=30 \times 10^{11}$  cm<sup>3</sup>s<sup>-1</sup> yielding an Auger lifetime of 2.3 ns at peak fluence. The density of emitting centers and the emission cross section that yield the best agreement with experimental data are respectively  $N=6 \times 10^{18}$  cm<sup>-3</sup> and  $\sigma=1.5 \times 10^{-17}$  cm<sup>2</sup>.

$$\begin{aligned}
 \frac{dN_1}{dt} &= -\sigma_p \phi_p(t) N_1 + \Gamma_{21} N_2 \\
 \frac{dN_2}{dt} &= \frac{N_3}{\tau} - \Gamma_{21} N_2 + B n_{ph} (N_3 - N_2) + (C_{A1} + C_{A2}) N_3^2 \\
 \frac{dN_3}{dt} &= -\frac{N_3}{\tau} - B n_{ph} (N_3 - N_2) + \Gamma_{43} N_4 - C_A N_3^2 \\
 \frac{dN_4}{dt} &= C_{A1} N_3^2 + \sigma_p \phi_p(t) N_1 - \Gamma_{43} N_4 \\
 \frac{dn_{ph}}{dt} &= V_a B n_{ph} (N_3 - N_2) - \frac{n_{ph}}{\tau_{ph}} + \beta \frac{N_3}{\tau_R}
 \end{aligned}
 \tag{1}$$

where  $N_i$  represent the level population densities ( $i=1, \dots, 4$ ),  $\sigma_p$  is the absorption cross section at the pump wavelength,  $\phi_p$  is the time dependent pumping photon flux,  $\Gamma_{ij}$  are the relaxation rates from the  $i$  to the  $j$  energy levels,  $\tau$  is the lifetime of the emitting level  $N_3$ ,  $B$  is the stimulated transition rate which implicitly contains the gain cross section  $\sigma$ ,  $n_{ph}$  is the number of emitted photons,  $V_a$  is the optical mode volume,  $\tau_{ph}$  is the photon lifetime,  $\beta$  is the spontaneous emission factor and  $\tau_R$  is the radiative lifetime of  $N_3$ .  $C_A$  is an effective Auger coefficient equal to  $2C_{A1} + C_{A2}$  if two different Auger processes are considered. The first consists of an electron relaxation

from level 3 to 2 with the energy given to a second electron which is excited from level 3 to higher lying levels from where it rapidly relaxes to the pumping level 4. This process involves two electrons in the same level: its rate depends quadratically through the coefficient  $C_{A1}$  on  $N_3$ . The other Auger mechanism involves an electron in level 3 and a hole in the valence band: the electron recombines while the hole is excited in the valence band and then very rapidly relaxes again. This process is proportional, through a coefficient  $C_{A2}$ , to the product of  $N_3$  and the hole concentration  $N_h$ ,  $N_h = N_2 + N_3 + N_4 \approx N_3$ , as the relaxation from levels  $2 \rightarrow 1$  and  $4 \rightarrow 3$  is so fast that levels 2, 4 are almost empty. As a general criterion, optical gain can be observed whenever the stimulated emission rate is greater than the Auger recombination rate [18]. Figure 3 reports experimental data and numerical calculations for the normalized luminescence decay as a function of the pumping rate. A fast recombination component builds up when the pumping rate is high enough to create population inversion. Because of the reduced propagation losses, in a time resolved luminescence experiment stimulated emission lifetimes can be measured at considerably lower fluencies than in TR-VSL (Fig. 2). On the other hand, since the effective photon propagation length is much smaller the rate of increase above threshold is weak. Good qualitative agreements are observed for a reasonable set of simulation parameters both at low and high pumping rates. Note that the agreements cannot be reached when stimulated emission is turned off, unless the Auger contribution is set extremely large: Auger lifetime of 50-70 ps at the peak photon flux. Within the four level recombination model it turned out that an emission (gain) cross section of the order of  $10^{-17} \text{ cm}^2$  is large enough to compensate for Auger processes with typical lifetimes as fast as 2-10 ns. It is interesting to note that the used Auger coefficients of about  $30 \times 10^{-11} \text{ cm}^3 \text{ s}^{-1}$ , when normalized over the Si-nc density yield an increased effective bulk Auger coefficient of  $\approx 10^{-29} \text{ cm}^6 \text{ s}^{-1}$  with respect to the accepted value for bulk Si of  $\approx 10^{-30} \text{ cm}^6 \text{ s}^{-1}$ , as expected for a low dimensional system.

Let us briefly comment on the nature of the involved four levels. X-ray absorption studies and ab-initio DFT calculations [19] suggest that Si-nc in  $\text{SiO}_2$  are coated by a 1 nm thick stressed silica shell. This stressed  $\text{SiO}_2$  could enhance the formation of oxygen-related states, like silanone bonds [9,10,20-22] at the interface between Si-nc and  $\text{SiO}_2$ . The energetic of silanone-like bond as a function of the Si=O interatomic distances is for Si-nc typical of a four level scheme, with different local surface atoms rearrangements for the Si-nc ground and excited state configurations, originating a significant Stokes shift between absorption and luminescence [10,20,21,23]. Within this scheme, photon excitation induces a strong structural relaxation of small H-saturated and O-saturated nanocrystals leading to new transitions involving surface localized states. In this picture levels 1 and 4 are associated with absorption transitions in the Si-nc ground state configuration while levels 2 and 3 are associated to the localized states in the excited state configuration. The broad and blue-shifted gain spectrum could be understood in terms of molecular-like inhomogeneous broadening mechanisms, such as different atomic surface configurations or strain fields, acting on small interface localized atoms or small silicon inclusions efficiently pumped by Si-nc through energy transfer. It remains clear however that accurate theories must still be developed for a detailed explanation of the relevant Si-nc gain physics.

## CONCLUSION

Optical gain dynamics has been studied in Si-nc samples. High power time-resolved luminescence and VSL measurements show the onset of stimulated emission with fast inversion

lifetime. A four-level model which includes amplified spontaneous emission and Auger processes has been introduced and a simple criterion for the occurrence of optical gain in Si-nc samples has been proposed. Good qualitative agreement with measured time-resolved decays has been obtained.

## ACKNOWLEDGMENTS

This work has been supported by INFM through the project RAMSES.

## References

1. P. Ball, *Nature* **409**, 974 (2001).
2. *Towards the first silicon laser*, edited by L. Pavesi, S. Gaponenko, L. Dal Negro, NATO Science Series (Kluwer Academic Publishers, Dordrecht 2003) in press.
3. L. Pavesi, L. Dal Negro, C. Mazzoleni, G. Franzò, F. Priolo, *Nature* **408**, 440 (2000).
4. L. Khriachtchev, M. Rasanen, S. Novikov, J. Sinkkonen, *Appl. Phys. Lett.* **79**, 1249 (2001).
5. M. Nayfeh, S. Rao, N. Barry, A. Smith, S. Chaieb, *Appl. Phys. Lett.* **80**, 121 (2002).
6. K. Luterova et al., *J. Appl. Phys.* **91**, 2896 (2002).
7. A. V. Malko et al., *Appl. Phys. Lett.* **81**, 1303, (2002)
8. V. I. Klimov et al., *Science* **290**, 314, (2000)
9. M. V. Wolkin, J. Jorner, P. M. Fauchet, G. Allan, C. Delerue, *Phys. Rev. Lett.* **82**, 197, (1999)
10. A. B. Filonov, S. Ossicini, F. Bassani, F. Arnaud d'Avitaya, *Phys. Rev. B* **65**, 195717, (2002)
11. F. Iacona, G. Franzò, C. Spinella, *J. Appl. Phys.* **87**, 1295 (2000).
12. K. L. Shaklee, R. E. Nahaory, R. F. Leheny, *J. Lumin.* **7**, 284 (1973).
13. L. Dal Negro et al., *Physica E* (2003), in press
14. J. Valenta, I. Pelant, J. Linnros, *Appl. Phys. Lett.* **81**, 1396 (2002).
15. P. W. Milonni, J. H. Eberly, "Lasers", John Wiley & Sons, New York 1988.
16. C. Delerue, M. Lannoo, G. Allan, *Phys. Rev. Lett.* **75**, 2228, (1995).
17. R. M'ghaieth, H. Maaref, I. Mihalcescu, J. C. Vial, *Phys. Rev. B* **60**, 4450, (1999).
18. A. A. Mikhailovsky, A. V. Malko, J. A. Hollingsworth, M. G. Bawendi, V. I. Klimov, *Appl. Phys. Lett.* **80**, 2380, (2002)
19. N. Daldosso et al., *Physica E* (2003) in press, M. Luppi, S. Ossicini, *phys. stat. sol. (a)* (2003) in press.
20. M. Caldas, *phys. stat. sol. (b)*, **217**, 641 (2000).
21. A. Puzder, A. J. Williamson, J. C. Grossman, G. Galli, *Phys. Rev. Lett.*, **88**, 097401 (2002).
22. F. Zhou, J. D. Head, *J. Phys. Chem. B*, **104**, 9981, (2000).
23. R. J. Baierle, M. J. Caldas, E. Molinari, S. Ossicini, *Solid State Comm.*, **102**, 545, (1997).